The authors acknowledge the valuable advice of Professor N. Kato of Meijoh University on this work. They thank Professors J. Harada and M. Sakata of Nagoya University who allowed the use of their program for calculating the thermal diffuse scattering. They also acknowledge Dr T. Abe of the Shin-Etsu Semiconductor Company for kindly supplying silicon wafers. They are indebted to Mr T. Little of the University of Illinois for a critical reading of the manuscript. This work was supported by a Grant in Aid of Scientific Research (no. 01580049, TT) from the Ministry of Education, Science and Culture of Japan to which the authors' thanks are due.

References

AL HADDAD, M. & BECKER, P. J. (1988). *Acta Cryst.* A**44**, 262-270.
BECKER, P. & AL HADDAD, M. (1990). *Acta Cryst.* A**46**, 123-129.
BECKER, P. & AL HADDAD, M. (1992). *Acta Cryst.* A**48**, 121-134.
BURAS, B. & GERWARD, L. (1975). *Acta Cryst.* A**31**, 372-374.
DARWIN, C. G. (1922). *Philos. Mag.* **43**, 800-829.
GRAF, H. A., SCHNEIDER, J. R., FREUND, A. K. & LEHMANN, M. S. (1981). *Acta Cryst.* A**37**, 863-871.
GUIGAY, J. P. (1989). *Acta Cryst.* A**45**, 241-244.
HAMILTON, W. C. (1957). *Acta Cryst.* **10**, 629-634.
HARADA, J. & SAKATA, M. (1992). Personal communication.
KATO, N. (1980*a*). *Acta Cryst.* A**36**, 763-769.
KATO, N. (1980*b*). *Acta Cryst.* A**36**, 770-778.
KATO, N. (1991). *Acta Cryst.* A**47**, 1-11.
OLEKHNOVICH, N. M., KARPEI, A. L., OLEKHNOVICH, A. I. & PUZENKOVA, L. D. (1983). *Acta Cryst.* A**39**, 116-122.
SAKA, T. & KATO, N. (1986). *Acta Cryst.* A**42**, 469-478.
SASAKI, S. (1989). KEK Report, Vol. 88-14, pp. 1-36. Photon Factory, Ibaraki, Japan.
SCHNEIDER, J. R., BOUCHARD, R., GRAF, H. A. & NAGASAWA, H. (1992). *Acta Cryst.* A**48**, 804-819.
SHIMURA, F. (1989). *Semiconductor Silicon Crystal Technology*. San Diego: Academic Press.
TAKAGI, S. (1962). *Acta Cryst.* **15**, 1311-1312.
TAKAMA, T., HARIMA, H. & SATO, S. (1990). *Acta Cryst.* A**46**, C412.
TAKAMA, T., IWASAKI, M. & SATO, S. (1980). *Acta Cryst.* A**36**, 1025-1030.
TAKAMA, T. & SATO, S. (1988). *Aust. J. Phys.* **41**, 433-448.
TAUPIN, D. (1964). *Bull. Soc. Fr. Mineral. Cristallogr.* **87**, 469-511.
VORONKOV, S. N., PISKUNOV, D. I., CHUKHOVSKII, F. N. & MAKSIMOV, S. K. (1987). *Sov. Phys. JETP*, **65**, 624-629.
WADA, K., INOUE, N. & KOHRA, K. (1980). *J. Cryst. Growth*, **49**, 749-752.
ZACHARIASEN, W. H. (1967). *Acta Cryst.* **23**, 558-564.

Acta Cryst. (1994). A**50**, 246–252

The Multiple-Diffraction Effect in Accurate Structure-Factor Measurements of PtP_2 Crystals

BY KIYOAKI TANAKA*

Chemistry Department, Nagoya Institute of Technology, Gokiso-machi Showa-ku, Nagoya 466, *Japan*

SHINJI KUMAZAWA, MICHIAKI TSUBOKAWA AND SIGEO MARUNO

Department of Electrical and Computer Engineering, Nagoya Institute of Technology, Gokiso-machi Showa-ku, Nagoya 466, *Japan*

AND ICHIMIN SHIROTANI

Department of Electrical Engineering, Muroran Institute of Technology, Mizumoto-cho 27-1, *Hokkaido* 050, *Japan*

(*Received* 26 *April* 1993; *accepted* 18 *August* 1993)

Abstract

Accurate X-ray intensities of a PtP_2 crystal were measured with the multiple-diffraction effect avoided by using the ψ rotation of the crystal around the scattering vector. The results were compared with those of a measurement made without avoiding the effect. The extinction parameters were more isotropic and the peaks of the deformation density were significantly smaller when multiple diffraction was avoided. In the measurement made without avoiding the effect, the number of structure factors affected by more than 1% was 403 from 936 reflections measured. Of 272 strong reflections with $\sin\theta/\lambda < 0.6$ Å^{-1} and $F_{obs} > 200$, 27 reflections were affected by more than 1%. These facts, as well as the smaller R values, indicate that the multiple-diffraction effect cannot be neglected in electron-density studies of crystals including heavy atoms. To assess the intensity fluctuation calculated in the present study, the intensities of 200 reflections were measured at intervals of 0.5° from 0 to 180° in ψ and compared with the calculated values. The variations of the measured and calculated intensities with ψ correspond to each other, which indicates that the present method can

* To whom correspondence should be addressed.

be used effectively to identify the reflections affected significantly by multiple diffraction.

Introduction

Many accurate measurements of electron densities have been carried out with careful consideration of the extinction effect while multiple diffraction (MD) has been neglected in most cases on the assumption that it occurs rarely. The probability of two reflections being located on the reflection sphere at exactly the same time is small if a well collimated incident beam with little energy width illuminates a very small crystal with no mosaic spread; however, since these conditions are not fulfilled, MD actually often occurs when the time lag between the two reflections touching the reflection sphere is small. We call the reflection that we are measuring the primary reflection and the reflection that touches the reflection sphere at approximately the same time the secondary reflection.

The intensity variation resulting from MD was formulated by Moon & Shull (1964) and was further modified to take into account the time lag (Tanaka & Saito, 1975) for a small crystal perfectly immersed in the incident beam. The time lag is defined in the following section. Tanaka (1978) applied the method to the electron-density study of *N*,*N*′-diformylhydrazide. The number of reflections affected in more than 1% of their structure factors was 62, of 4532 reflections, and the deformation densities calculated from reflections before and after the correction for MD showed a little difference. We have recently studied the electron densities of crystals including heavy atoms: BaClF (Kodama, Tanaka, Utsunomiya, Hoshino, Marumo, Ishizawa & Kato, 1984) and PtP_2 (Tanaka, Kumazawa, Maruno & Shirotani, 1994). In all these studies, large peaks remained on the residual density maps around the heavy atoms after the analysis of orbital functions and anharmonic vibrations, indicating that errors of unknown origin still exist in our intensity measurements. The present study was undertaken to establish the method of intensity measurement at ψ with minimum MD effect and to show the importance of the effect in accurate intensity measurements of crystals including heavy atoms. A program was written for this purpose. The method was applied to the intensity measurement of a pyrite-type crystal, PtP_2. The results are compared with those of a refinement performed using the intensities measured with the conventional method.

Theoretical

1. *Intensity variation caused by multiple diffraction*

This was first formulated by Moon & Shull (1964) and was modified by Tanaka & Saito (1975) as follows:

$$\Delta I_1/I_1 = (4\pi)^{-1} Q_{01} \sum_i [-g_{01;0i}(Q_{0i}/Q_{01})T_0 - g_{01;1i}(Q_{1i}/Q_{01})T_1 + g_{0i;i1}(Q_{0i}/Q_{01})(Q_{i1}/Q_{01})T_i], \quad (1)$$

where the suffix 0 indicates the incident beam from the source and the suffixes 1 and $i(>1)$ indicate the primary and ith secondary beams, diffracted by the planes $\mathbf{H}_{01}$ and $\mathbf{H}_{0i}$, respectively. The geometrical relations and the notation of the planes are the same as those in Fig. 1 of Moon & Shull (1964). The suffix ij indicates that the beam i acts as the incident beam to the plane $\mathbf{H}_{ij} = \mathbf{H}_{0j} - \mathbf{H}_{0i}$ and is diffracted as the beam j. T_0, T_1 and T_i are the absorption-weighted mean path lengths defined by Becker & Coppens (1974*a*) of the incident, primary and secondary beams, respectively. ΔI_1 is the variation of the primary-beam intensity I_1 due to MD. Q_{ij} is the integrated reflectivity per unit volume of the crystal. $g_{ij;kl}$ is a constant relevant to the diffraction processes ij and kl in which the effect of the time lag on ΔI_1, the difference between the primary and secondary reflections, is taken into account. The explicit form is

$$g_{ij;mn} = (p_{ij}/\eta_{ij})(p_{mn}/\eta_{mn}) \times f[K_{ij}^2/(2\eta_{ij})^2, K_{mn}^2/(2\eta_{mn})^2], \quad (2)$$

where K_{ij} is the constant that transforms the rotation angle of the crystal to that of the Bragg angle θ. The term p_{ij} is the polarization factor of the diffraction process ij and η_{ij} is expressed in terms of the full width at half-maximum (FWHM) x_{ij} of the reflection $\mathbf{H}_{ij}$ as

$$\eta_{ij} = x_{kj}/(8 \ln 2)^{1/2} \quad (3)$$

and

$$f(a, b) = [\pi/(a + b)]^{1/2} \exp[-ab/(a + b)\zeta^2]. \quad (4)$$

The parameter ζ expresses the time lag in terms of the rotation angle of the crystal, *i.e.* the crystal needs to be rotated by ζ for the secondary reflection to be positioned exactly on the reflection sphere after the primary reflection had been exactly on the reflection sphere.

The first term in (1) corresponds to the diminution of the primary beam owing to the decrease in intensity of the incident beam caused by the secondary reflection i. The second term also indicates the diminution of the primary beam, which is diffracted again by the $\mathbf{H}_{0i} - \mathbf{H}_{01}$ plane towards the direction of the secondary beam i. The third term gives the increase in the intensity of the primary beam by the opposite process to that in the second term. For crystals with heavy atoms, values of Q_{ij} are large so the intensity variation caused by MD is expected to be significantly enhanced. MD is expected to be one

Table 1. *Crystal data at* 298 K

Space group	*Pa*3
a	5.69485 (4) Å
V	184.691 (4) Å^3
Z	4
D_x	9.260 g cm^{-3}
μ (Mo $K\alpha$)	781 cm^{-1}
$F(000)$	372

of the main sources of error in the structure-factor measurements of crystals including heavy atoms. As pointed out by Moon & Shull (1964), the error can be comparable with that caused by the extinction effect.

2. *Peak-shape approximation*

Since ΔI_1 in (1) depends acutely on the FWHM defined in (3) and since the FWHM can also be utilized for the discrimination of the effective secondary reflections as described in the following section, the value of the FWHM of each reflection is necessary for the evaluation of ΔI_1. In the MXC3 four-circle diffractometer (MAC Science) used in the present study, the continuous-scan method is employed for the measurement; however, the diffractometer actually measured intensities with the step-scan method and the number of counts n_i of each step is stored on a disk. An n_i normalized to the counts in 1 s was used to calculate the parameters that express the Gaussian-type peak shape described as

$$n_i = 2a \exp[-b(\omega_i - \omega_0)^2] + a \exp[-b(\omega_i - \omega_0 - \omega_{12})^2], \quad (5)$$

where i runs from 1 to N, the number of steps, ω_0 and $\omega_0 + \omega_{12}$ are the ω angles at the tops of the peaks of $K\alpha_1$ and $K\alpha_2$ radiations, respectively, and ω_i is the ω angle of the ith step. The factor 2 is applied to take the intensity ratio of 2 to 1 of the $K\alpha_1$ and $K\alpha_2$ radiations into account. The FWHMs of the peaks of the two radiations were assumed to be the same and a symmetrical peak profile was assumed. The parameters a and b were calculated by the least-squares method. x_{01} in (3) is calculated as

$$x_{01} = (4 \ln 2)^{1/2}/b. \quad (6)$$

Experimental

Crystals of PtP_2 were synthesized under high pressure, 2.5 GPa, at 827 K (Shirotani, 1982). The crystal data are summarized in Table 1. In order to calculate accurately the orientation matrix of the crystal, 2θ angles of 173 reflections with 2θ ranging from 61.85 to 84.24° for Mo $K\alpha_1$ radiation were measured after adjustment of the incident-beam path at the optimum position. Since the linear absorption coefficient is very large, a crystal was shaped into a sphere with diameter 0.10 mm by the Bond (1951) method as improved by Kato (1975).

1. *Measurement of integrated intensities of* 200 *with* ψ *scan*

The structure factor $F_{obs}(200)$ of the PtP_2 crystal was measured from $\psi = 0$ to $\psi = 180°$ at intervals of 0.5°. The fluctuation of the structure factor, δF_i, caused by the ith secondary reflection is calculated using (1). Since the Gaussian function has a long tail at each side of the peak, the initial criterion

$$\zeta < x_{01} + x_{0i} \quad (7)$$

is necessary to identify the ineffective secondary reflections that erroneously make $|\delta F_i|$ values too large. As in the previous study (Tanaka & Saito, 1975), reciprocal points are assumed to have finite sizes instead of the surface of the reflection sphere. An isotropic peak profile is also assumed in (7) and the x_{0i} calculated by the least-squares analysis of n_i's, given by (5), measured on the horizontal plane is used. The second criterion is expressed in terms of δF_i, F and its statistical counting error σF by

$$|\delta F_i| > \sigma F \quad \text{or} \quad |\delta F_i| > 0.001|F|. \quad (8)$$

If a secondary reflection fulfils conditions (7) and (8), it is judged effective and δF_i is summed as

$$\Delta F = \sum_i \delta F_i. \quad (9)$$

The unscaled value of $F_{obs}(200)$ at each ψ is illustrated in the upper curve of Fig. 1 with the factor C defined in the lower curve by

$$F_{cor} = (1 + \Delta F/F_{obs})F_{obs} = CF_{obs}, \quad (10)$$

where F_{cor} is the structure factor corrected for MD. The numbers of significant secondary reflections that fulfil the criteria are shown in Fig. 2. It is evident that MD cannot be completely avoided at any ψ position. Since the unit cell of the PtP_2 crystal is very

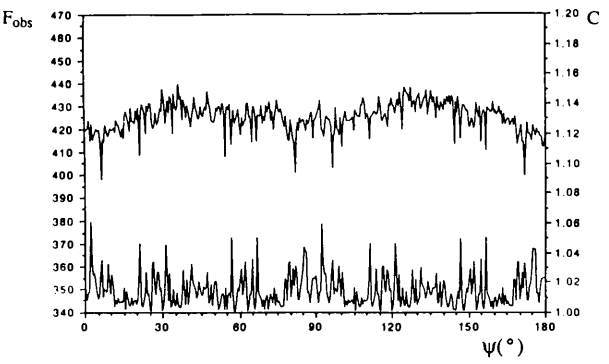

Fig. 1. Observed structure factors $F_{obs}(200)$ measured at $\psi = 0$ to 180° at intervals of 0.5° (upper curve) and the calculated correction factor C (lower curve).

small, it can be concluded that MD cannot be avoided in general. Therefore, the problem we should consider is whether the intensity variations caused by MD are significant or not compared with errors from other sources, such as statistical counting errors.

2. *Intensity measurement with multiple diffraction avoided*

The intensity measurements made with MD avoided [experiment (I)], as well as the conventional ones [experiment (II)], were carried out using the MXC3 four-circle diffractometer. Intensities of reflections with 2θ up to 150 and 130° were measured in experiments (I) and (II), respectively, employing an ω–2θ scan with scan speed 2° min^{-1} in ω. The total numbers of reflections measured in (I) and (II) were 2125 and 1712, respectively. The strongest ten reflections and all of their equivalent reflections were measured to correct for the anisotropic extinction effect. The two measurements were made using the same crystal under the same conditions except for the 2θ range. The experimental conditions are summarized in Table 2.

Table 2. *Experimental conditions*

Crystal shape	Spherical
Diameter	0.10 mm
Scan mode	ω 2θ
Receiving slits	
Vertical	1.5
Horizontal	1.5
2θ range	
Experiment (I) (MD avoided)	0 155
Range of h	−8 15
Range of k	8–15
Range of l	−8 15
Experiment (II) (MD not avoided)	0 130
Range of h	−8 14
Range of k	8–14
Range of l	−8 14
No. of significant reflections ($F > 3\sigma F$)	
Experiment (I)	986
Experiment (II)	865
No. of reflections used ($2\theta < 130$)	
Refinement (I*a*)	919
Refinements (I*b*) and (II*b*)	823
Refinement (II*a*)	873
No. of independent reflections	
Refinement (I*a*)	267
Refinements (I*b*) and (II*b*)	249
Refinement (II*a*)	255

The program *IUANGLE* was originally part of the machine-control program system used to calculate the four angles for the intensity measurement. It was modified by SK and KT to calculate the intensity fluctuation due to MD at each ψ angle, and supplies the most appropriate four angles to the diffractometer. Experiment (I) was carried out with the following procedures.

(*a*) The present method requires a set of structure factors or Q_{01} values of independent reflections before the measurement. Q_{01} values were calculated using the atomic parameters determined in the preliminary measurement.

(*b*) After the orientation of the crystal was determined, the itensity variation ΔI_1 due to MD was calculated using (1). The calculations were carried out separately for $K\alpha_1$ and $K\alpha_2$ radiations and the corresponding results are designated ΔI_{11} and ΔI_{12}, respectively. The total intensity variation was calculated with the following equation by assuming the $K\alpha_1$ and $K\alpha_2$ radiations to be incoherent:

$$\Delta I_1 = \tfrac{1}{3}(2\Delta I_{11} + \Delta I_{12}). \qquad (11)$$

(*c*) The calculation of ΔI_1 was continued with ψ shifted by 1° until $\Delta I_1/I_1$ became less than 0.002 and the intensity was measured. If this condition was not fulfilled after 360° of ψ rotation, $|\Delta I_1|$ was calculated at intervals of 0.1° at both sides of the ψ with the minimum $|\Delta I_1|$. The intensity was measured at the ψ with the smallest $|\Delta I_1|$ among the further-divided ψ angles.

(*d*) Some areas of reciprocal space cannot be scanned and are here referred to as the blind regions.

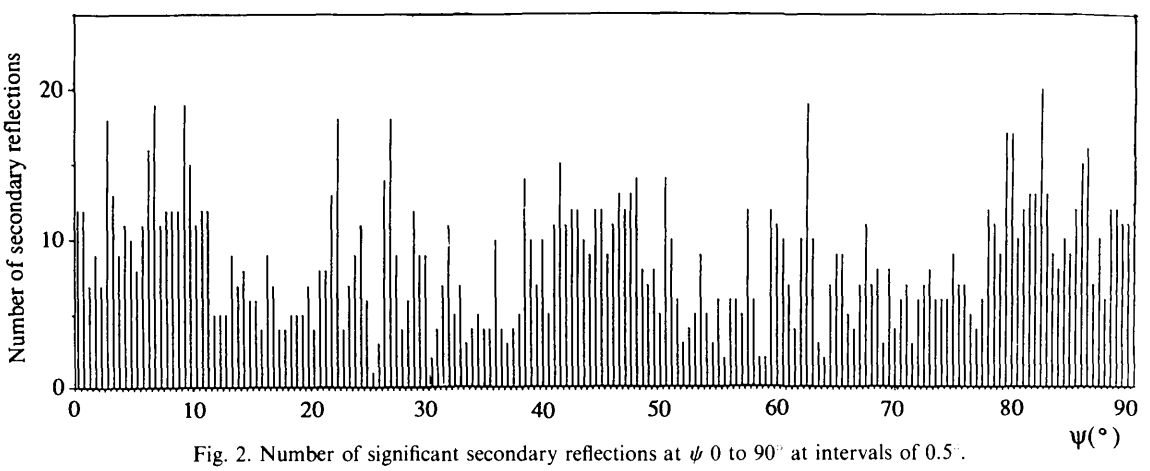

Fig. 2. Number of significant secondary reflections at ψ 0 to 90° at intervals of 0.5°.

Table 3. *Multiple-diffraction effect on* PtP_2 *crystals*

For all the observed 936 reflections
Number of reflections with $\delta F > \sigma F$: 327
Number of reflections with $\Delta F > \sigma F$: 340
Number of reflections affected more than x%:

x	10	5	1	0.5	0.1
A ($\delta F/F$)	17	45	281	568	922
B ($\Delta F/F$)	30	59	353	454	653
A and B	17	44	231	404	653
A or B	30	60	403	618	922

For 272 low-order ($\sin\theta/\lambda < 0.6$ Å^{-1}) and strong* ($F_{obs} > 200.0$) reflections
Number of reflections with $\delta F > \sigma F$: 69
Number of reflections with $\Delta F > \sigma F$: 65
Number of reflections affected more than x%:

x	10	5	1	0.5	0.1
A ($\delta F/F$)	0	0	12	60	184
B ($\Delta F/F$)	0	0	21	46	138
A and B	0	0	6	22	138
A or B	0	0	27	84	184

* Maximum F_{obs} = 393.3 for 200.

Table 4. *Fractional coordinates and thermal parameters* (Å^{-2}) *and type-*I *extinction parameters*

Multiple diffraction was avoided for data sets (I*a*) and (I*b*) and not avoided for data sets (II*a*) and (II*b*).

	(I*a*)	(I*b*)	(II*a*)	(II*b*)
Platinum				
U_{11}	0.00195 (2)	0.00195 (2)	0.00199 (2)	0.00202 (2)
U_{12}	−0.00010 (3)	−0.00009 (3)	−0.00014 (4)	−0.00011 (4)
Phosphorus				
x	0.38952 (9)	0.38952 (9)	0.38950 (11)	0.38950 (10)
U_{11}	0.00304 (8)	0.00319 (9)	0.00316 (10)	0.00330 (10)
U_{12}	0.00010 (14)	0.00002 (14)	0.00013 (17)	0.00013 (17)
Type-I anisotropic-extinction parameters				
Z_{11}	0.00197 (10)	0.00198 (10)	0.00200 (12)	0.00220 (12)
Z_{22}	0.00224 (22)	0.00228 (22)	0.00289 (30)	0.00293 (29)
Z_{33}	0.00203 (12)	0.00204 (11)	0.00259 (16)	0.00267 (16)
Z_{12}	−0.00018 (12)	−0.00018 (12)	0.00011 (15)	0.00013 (15)
Z_{13}	−0.00016 (9)	−0.00016 (9)	−0.00029 (11)	−0.00011 (12)
Z_{23}	0.00014 (15)	0.00013 (15)	−0.00012 (20)	−0.00013 (19)
R	0.0122	0.0114	0.0142	0.0130
R_w	0.0133	0.0126	0.0158	0.0146

The blind regions were specified in the replaceable subroutine *BLIND* for the MXC3 diffractometer. The angles used in the measurement were calculated by taking the scan range and the width of the receiving slits into account.

The effects of MD on PtP_2 intensities calculated in experiment (II) are summarized in Table 3.

Refinement

The crystal structure was refined with the two sets of intensities measured in experiments (I) and (II) for reflections with $2\theta < 130°$. If more than half of the equivalent reflections had structure factors smaller than $3\sigma(F)$, all the equivalent reflections were taken as insignificant and were deleted. The set of reflections selected in this way from those measured in experiment (II) is called data set (II*a*). Data set (II*a*) is the one usually measured with no consideration of the effect of MD. Some of the high-order reflections measured in experiment (I) have only a little room for ψ rotation because of the blind regions and MD could not be avoided. Reflections were judged to be affected by MD if $|\delta F|$ and $|\Delta F|$ in (9) satisfied one of four conditions: (*a*) $|\Delta F| > 6\sigma F$, (*b*) $|\delta F|/|F| > 0.1$, (*c*) $|\Delta F|/|F| > 0.1$, (*d*) $|F| > 100.0$ and $|\Delta F|/|F| > 0.01$. Condition (*d*) was added to eliminate the strong low-order reflections affected by MD. For strong reflections, the fluctuation of 1% in F is still larger than $3\sigma(F)$. Since the extinction effect is prominent in only a limited number of strong low-order reflections, the extinction parameters calculated by the least-squares method without condition (*d*) are affected significantly. The set of reflections thus obtained from experiment (I) is called data set (I*a*) and is almost free of the effects of MD. To compare more precisely the effects of MD on the intensities measured in experiments (I) and (II), data sets (I*b*) and (II*b*) were prepared from only those reflections existing in both data sets (I*a*) and (II*a*).

Scattering factors and anomalous-dispersion terms of platinum and phosphorus were taken from *International Tables for X-ray Crystallography* (1974). Refinement with the assumption of a type-I anisotropic extinction effect gave lower R factors than refinement with the assumption of a type-II effect. The final atomic parameters, those of type-I anisotropic extinction (Becker & Coppens, 1974*a*,*b*, 1975) and R factors are listed in Table 4.* The refinements were carried out with the program *LINKT*80, coded by KT. The deformation densities are shown in Figs. 3(*a*) and (*b*). Further analysis of the electron density of PtP_2 will be published elsewhere (Tanaka, Kumazawa, Maruno & Shirotani, 1994).

Results and discussion

Fig. 1 clearly shows the $F_{obs}(200)$ are affected by the anisotropic extinction effect, which makes F_{obs} vary gradually with ψ, and by the effect of MD, which makes the variation of F_{obs} with ψ sharp. The correspondence between the two curves in Fig. 1 is quite high since the decrease of F_{obs} everywhere corresponds to the increase of C in (10); however, their values do not seem to agree very well with each other. The reasons are that (1) is based on (9) as formulated by Moon & Shull (1964) for a flat-plate crystal with low absorption and extinction effects

* Lists of structure factors for the four refinements have been deposited with the British Library Document Supply Centre as Supplementary Publication No. SUP 71511 (33 pp.). Copies may be obtained through The Technical Editor, International Union of Crystallography, 5 Abbey Square, Chester CH1 2HU, England.

and that the energy transfer among the secondary reflections is neglected in the present method. Therefore, the present method was used as a practical and effective measure to judge the occurrence of MD.

The parameters a, b and ω_0 in (5) were determined for each reflection by the least-squares method with the program *TEST*, coded by MT. They are listed in Table 5 for 200 and 10,0,0. The peaks of 10,0,0 are split into those for $K\alpha_1$ and $K\alpha_2$ radiations. The mean values of these parameters for all the reflections having peak shapes clear enough for the parameters to be evaluated are also listed in Table 5. FWHMs calculated from the measured peak shapes are used in the subsequent calculation of ΔI_1. For the other reflections, the mean value of 0.230° was used. The reliability factor $R_p = \sum n_{i,\mathrm{obs}} - n_{i,\mathrm{calc}} / \sum n_{i,\mathrm{obs}}$ for each reflection was approximately 0.1. Most of the discrepancies come from the non-coincidence at both sides of the peak. After use of the measured FWHM and elimination of the secondary reflections with (7), all the C values less than 1.0 in (10) disappeared and the coincidence of C and the fluctuation of $F_{\mathrm{obs}}(200)$ was improved.

Table 5. *Parameters of peak profiles of* 200 *and* 10,0,0 *and the mean values calculated from the parameters of all the reflections with clear peak shapes*

h	k	l	a	b	ω_0(°)	FWHM (°)	R_p
2	0	0	713	43.7	0.620	0.252	0.117
10	0	0	107	42.2	0.663	0.211	0.096
Mean value				43.0	0.683	0.230	

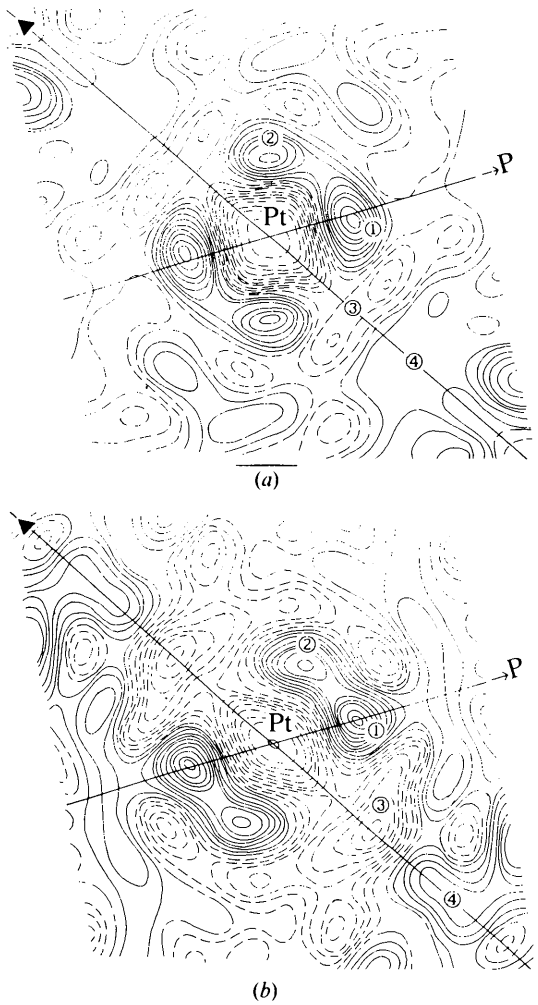

Fig. 3. Deformation densities on the plane defined by the threefold axis and the line from platinum to the nearest-neighbour phosphorus (*a*) after refinement (I*a*) (MD avoided) and (*b*) after refinement (II*a*) (MD not avoided). The contours are at intervals of 0.2 e Å^{-3}. Negative contours are broken lines and the zero contours are dash-dotted lines.

The effect of MD in experiment (II) is summarized in Table 3. About 36% of reflections are affected by MD more than their estimated standard deviations (e.s.d.'s). For low-order strong reflections with $\sin\theta/\lambda < 0.6$ Å^{-1} and $F_{\mathrm{obs}}| > 200$, the ratio is still as high as 25%. Since $\Delta I_1/I_1$ in (1) is proportional to Q_{01}, the effect of MD becomes larger in general as the crystal contains heavier atoms. The range of the ratios of Q values in (1) is also larger. This is the reason why 60 reflections were affected by MD in more than 5% of their structure factors. The R factor in the present study is 0.012 for refinement (I*a*) and the number of reflections affected by MD by more than 1% is 403 from 936 observed reflections. These facts indicate that MD cannot be neglected for crystals including heavy atoms and should be avoided as far as possible.

It is very interesting to compare the parameters determined in refinements (I*a*), (I*b*), (II*a*) and (II*b*) in Table 4. The x coordinate of phosphorus and most of the thermal parameters except U_{11} of phosphorus agree within their e.s.d.'s. Since a significant number of the low-order reflections are affected by MD, the refinements of the two sets of intensity data measured in experiments (I) and (II) are expected to give different extinction parameters. In fact, the type-I anisotropic extinction parameters Z_{22} and Z_{33} are significantly different. Refinements (I*a*) and (I*b*) give almost isotropic extinction parameters, that is, Z_{11}, Z_{22} and Z_{33} are almost equal within their e.s.d.'s and off-diagonal parameters are very small. It becomes evident that MD affects significantly extinction parameters and thus electron-density maps.

Deformation densities produced after the refinements with data sets (I*a*) and (II*a*) are shown in Figs. 3(*a*) and (*b*), respectively. Discrepancies between the figures are quite clear and the differences between the observed and calculated electron densities are in general smaller in (*a*) than in (*b*). The peaks ① on the Pt–P bonds in (*a*) and (*b*) are 1.6 and 2.2 e Å^{-3} in height, respectively. The heights of the peaks ② at the bisecting position of the two lines in

(*a*) and (*b*) are 1.3 and 1.5 e Å $^{-3}$, respectively. The position of the peak in (*a*) is slightly shifted towards the threefold axis compared with that in (*b*). The trough ③ on the threefold axis is as deep as -1.6 e Å $^{-3}$ in (*b*), but is shallow in (*a*). The height of the peak ④ on the axis in (*b*) is 0.9 e Å^{-3}, while the height at the corresponding position in (*a*) is 0.4 e Å $^{-3}$. The depth of the trough at platinum is -2.1 e Å $^{-3}$ in both figures. Since the differences between (*a*) and (*b*) are caused by MD, these parts of the electron density in (*b*) cannot be fully represented by models of electron-density distributions or of thermal vibrations. Therefore, the intensity data that are not affected by MD should be collected or the effect of MD should be corrected for before analyses of electron densities, atomic orbitals and thermal vibrations.

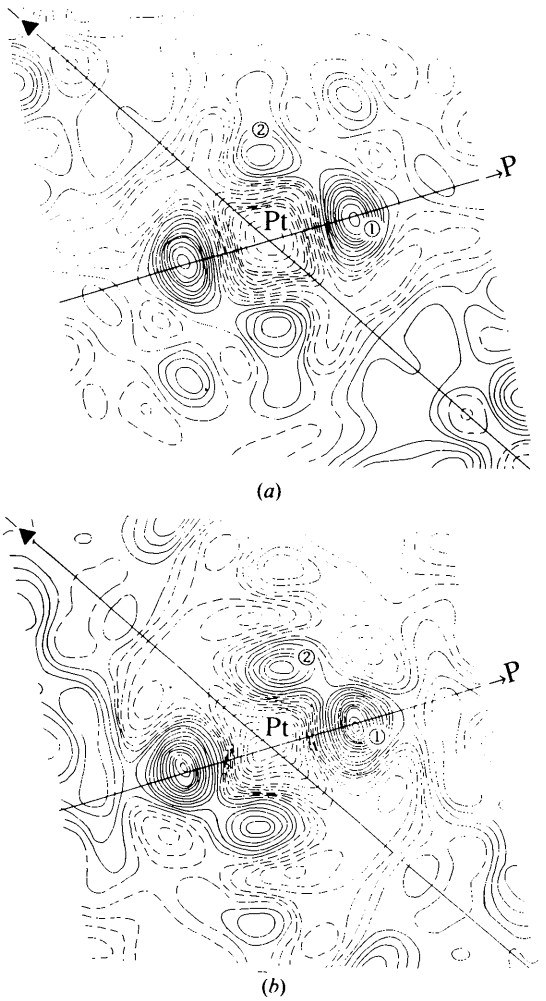

Fig. 4. Deformation densities on the same plane as in Fig. 3. (*a*) After refinement (I*b*) (MD avoided) and (*b*) after refinement (II*b*) (MD not avoided). The countours are as in Fig. 3.

Deformation densities of the refinements of data sets (I*b*) and (II*b*) are illustrated in Figs. 4(*a*) and (*b*). These data sets are composed of the same number of reflections with the same indices. The heights of the peaks ① on the Pt–P bonds in (*a*) and (*b*) are 2.3 and 2.6 e Å^{-3}, respectively. Peaks ② at the bisecting position have heights of 0.9 and 1.4 e Å^{-3} in (*a*) and (*b*), respectively. The troughs ③ on the threefold axis in Fig. 3(*b*) do not exist in Figs. 4. The troughs at platinum in Figs. 4(*a*) and (*b*) have depths of -2.5 and -2.1 e Å^{-3}, respectively. Very weak high-order reflections, which are affected by MD much more appreciably than low-order reflections because of the larger ratio of Q values in (1), can hardly remain in both data sets as significant, so the differences between the two parts of Fig. 4 are not as prominent as those between the parts of Fig. 3. However, the results of the measurements avoiding MD still show, in general, smaller peaks and troughs.

The authors express their sincere gratitude to Mr Hironao Inoue and Dr Chuji Katayama of MAC Science for the cooperation in installing *IUANGLE* in the machine-control program system of the MXC3 diffractometer. Support from the Research Foundation for Electrotechnology of Chubu and from the Izumi Science and Technology Foundation is gratefully acknowledged. This work has been partly supported by a Grant in Aid of Scientific Research from the Ministry of Education, Science and Culture of Japan.

References

BECKER, P. J. & COPPENS, P. (1974*a*). *Acta Cryst.* A**30**, 129–147.
BECKER, P. J. & COPPENS, P. (1974*b*). *Acta Cryst.* A**30**, 148–153.
BECKER, P. J. & COPPENS, P. (1975). *Acta Cryst.* A**31**, 417–425.
BOND, W. L. (1951). *Rev. Sci. Instrum.* **22**, 344.
International Tables for X-ray Crystallography (1974). Vol. IV. Birmingham: Kynoch Press. (Present distributor Kluwer Academic Publishers, Dordrecht.)
KATO, M. (1975). Private communication.
KODAMA, N., TANAKA, K., UTSUNOMIYA, T., HOSHINO, Y., MARUMO, F., ISHIZAWA, N. & KATO, M. (1984). *Solid State Ionics*, **14**, 17–24.
MOON, R. M. & SHULL, C. G. (1964). *Acta Cryst.* **17**, 805–812.
SHIROTANI, I. (1982). *Mol. Cryst. Liq. Cryst.* **86**, 203–212.
TANAKA, K. (1978). *Acta Cryst.* B**34**, 2487–2494.
TANAKA, K., KUMAZAWA, S., MARUNO, S. & SHIROTANI, I. (1994). In preparation.
TANAKA, K. & SAITO, Y. (1975). *Acta Cryst.* A**31**, 841–845.